Eur. Phys. J. B **62**, 45–51 (2008)
DOI: 10.1140/epjb/e2008-00117-x

THE EUROPEAN PHYSICAL JOURNAL B

Spin-dependent shot noise in diluted-magnetic-semiconductor/semiconductor heterostructures

Y. Guo[a], L. Han, R. Zhu, and W. Xu

Department of Physics and Key Laboratory of Atomic and Molecular NanoSciences, Ministry of Education, Tsinghua University, Beijing 100084, P.R. China

Received 24 July 2007 / Received in final form 1st February 2008
Published online 19 March 2008 – © EDP Sciences, Società Italiana di Fisica, Springer-Verlag 2008

Abstract. We investigated the shot noise properties in the diluted-magnetic-semiconductor/semiconductor heterostructures, where the *sp-d* exchange interaction gives rise to a giant spin splitting when an external magnetic field is applied along the growth direction of the heterostructures. It is found that the noise becomes strongly spin-dependent and can be greatly modulated not only by the external magnetic and electric fields, but also by the structural configuration and geometric parameters. Both the spin-up and spin-down components of the noise spectral density can be greatly suppressed by the magnetic field. The Fano factor is notably sensitive to the transmission probabilities, which varies greatly with the spin-polarization, the external magnetic field, and the structural configuration.

PACS. 73.50.Td Noise processes and phenomena – 75.50.Pp Magnetic semiconductors – 72.25.-b Spin polarized transport

1 Introduction

In recent years, spin-dependent transport in semiconductor environments has been one of the most important issues in the field of spintronics, where spin-related effects are of central importance in the realization of electronic devices with new functions [1–3]. The Mn-based diluted-magnetic-semiconductor (DMSs), typically (II, Mn)VI and (III, Mn)V DMSs, are prospective candidates for the materials that combine semiconductor behaviors with robust magnetism in application to spintronics devices [4–11]. There has been great theoretical and experimental progress made in spin transport through these and other diluted-magnetic semiconductor systems. Sugakov and Yatskevich [12] earlier examined spin splitting in parallel electric and magnetic fields through a double-barrier heterojunction using a transfer-matrix method. Egues [13] investigated spin-dependent transport through a ZnSe/$Zn_{1-x}Mn_xSe$ heterostructure with a single paramagnetic layer and found strong spin filtering effect. One of us and our coauthors [14] have demonstrated several effects on spin-polarized transport, such as the electric field effect, spin-dependent resonant enhancement and suppression effects, spin-dependent splitting effect, spin separation on the time scale, etc. Béjar, Sánchez, and Papp analyzed spin transport and spin dynamics in the similar DMS/S systems [15]. Li et al. [9] theoretically investigated the spin-dependent transport through $Cd_{1-x}Mn_xTe$ DMS quantum dots under the influence of both the external electric and magnetic fields using the recursion method and predicted 100% polarized electric current by using suitable structure parameters. Chang and Peeters explored the energy dispersion of an electron in DMS double quantum wire consisting of $Zn_{1-x}Cd_xSe$ wires separated by a DMS barrier $Zn_{0.9}Mn_{0.1}Se$ and found that it is spin-dependent and modified significantly by an external magnetic field [16]. While most of the researches in this field focus on time-averaged quantities of the system (e.g., the spin-polarized current and conductance), relatively less study has focused on the time-dependent properties, such as the shot noise.

Fluctuations in time of a measurement offer much information, which is not provided by the time-averaged quantities. Shot noise, a non-equilibrium current fluctuation due to the quantization of the charge, is useful to obtain information on a system which is not available through conductance measurements [17]. In particular, shot noise experiments can determine the quantum correlation of electrons, the charge and statistics of the quasi-particles relevant for transport, and reveal information on the potential profile as well as internal energy scales of mesoscopic systems. An example is the determination of quasiparticle charge in the fractional

[a] e-mail: guoy66@tsinghua.edu.cn

quantum Hall effect [18] by measuring both the power of shot noise $S = 2Q\bar{I}_e$ and the average electric current $\bar{I}_e$, deducing $Q = e/3$. Similarly, for charge-current correlation in normal-superconductor tunnel junctions, measurements [19] of shot noise determine $Q = 2e$, the charge of Cooper pairs. More recently, the study of spin-polarized noise has attracted growing attention [20–26]. Considering spin-related effects, shot noise is also a useful probe for detecting entanglement. Based on a beam splitter with spin-orbit interaction in one of the incoming leads, it was found that spin polarization and entanglement can be observed through shot noise measurements [27,28]. The contribution of the spin-flip scattering to the shot noise in a spin-resolved tunneling system was also considered by Brito and Egues [29]. The noise properties of quasi-one-dimensional nanowires with Rashba spin-orbit coupling effect under an external magnetic field have been investigated by Li et al. [30] The noise of the considered system is found to be strongly spin-dependent.

In this paper, we study the noise properties in the symmetric and asymmetric diluted-magnetic-semiconductor/semiconductor heterostructures in the presence of both electric and magnetic fields. The results indicate that the noise is substantially spin-dependent in the considered system and can be greatly modulated by the electric and magnetic fields and the structural configuration.

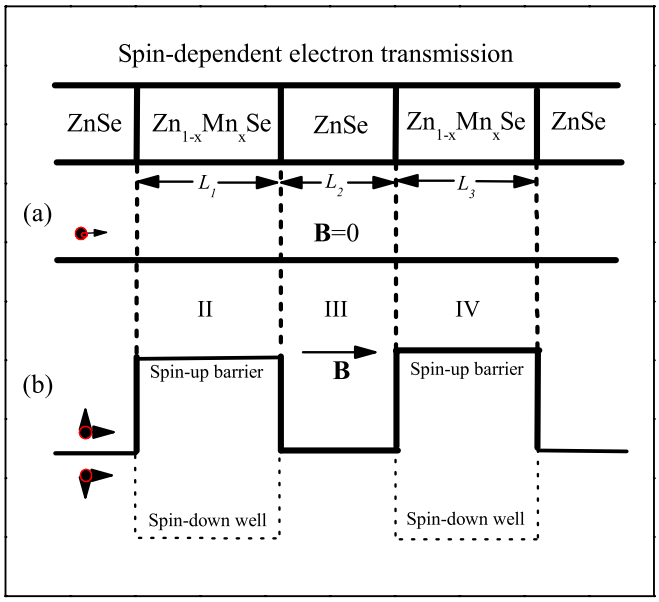

Fig. 1. $ZnSe/Zn_{1-x}Mn_xSe$ multilayers and their conduction-band profile. (a) Zero band offsets potential in the absence of a magnetic field; (b) spin-up electrons see a double-barrier potential while spin-down electrons see a double-well potential under certain applied magnetic field [14].

2 Method

We consider the $ZnSe/Zn_{1-x}Mn_xSe/ZnSe/Zn_{1-x}Mn_x \times Se/ZnSe$ heterostructure, where electrons interact with the three-dimensional electrons of the localized magnetic moments of the Mn ions via the *sp-d* exchange interaction. Figure 1 shows the conduction-band profile of the multilayer heterostructure under consideration. Within the molecular-field approximation and for a magnetic field B along the z axis (defined along the growth direction), it can be described by a spin-dependent potential $V_{\sigma_z} = -N_0\alpha\hat{\sigma}_z x_{eff} \langle S_z \rangle$ in the two paramagnetic layers. Here $N_0\alpha$ is the electronic *sp-d* exchange constant, which varies with the Mn concentration. σ_z is the electronic spin component $\pm 1/2$ along the field. $x_{eff} = x(1-x)^{12}$ is the effective Mn concentration, while x accounts for the real Mn concentration. $\langle S_z \rangle$ is the thermal average of the z component of the Mn^{2+} spin which is given by the modified 5/2 Brillouin function $(5/2)B_{5/2}(5\mu_B B/k_B T_{eff})$. Here $T_{eff} = T + T_0$ is the effective temperature in which T_0 denotes the Mn-Mn interaction at $T = 0$ K. In the absence of any kind of electron scattering, the motion along the z axis is decoupled from that of the $x-y$ plane. The in-plane motion is quantized in Landau levels with energies $E_n = (n+1/2)\hbar\omega_c$, where $n = 0, 1, 2, \cdots$ and $\omega_c = eB/m_e^*$ (we assume a single electron mass m_e^* throughout the heterostructure). Therefore, the motion of the electrons can be reduced to a one-dimensional problem along the z axis, that can be modeled by the following Hamiltonian

$$\hat{H} = -\frac{\hbar^2}{2m_e^*}\nabla^2 + V_0(z) + V_{\sigma_z}(z) + V_s. \tag{1}$$

Here $V_0(z) = -eFz\Theta(z)\Theta(L_1 + L_2 + L_3 - z)$ is the zero magnetic-field conduction band offset, where F is the magnitude of the electric field, which is assumed to be homogeneous in the whole heterostructure region, $\Theta(z)$ is the step function, and 0, L_1, L_1+L_2, $L_1+L_2+L_3$ are the longitudinal coordinates of surfaces in z direction. $V_s = \frac{1}{2}g_s\mu_B\hat{\sigma}_z B$ is the Zeeman splitting of the electron.

The spin-dependent wave functions for the electrons can be obtained from the Schrödinger equation based on the Hamiltonian (1), that can be written as follows

$$\psi_\sigma(\mathbf{r}) = \exp(i\mathbf{k_{xy}}\rho) \times \begin{cases} \left[\sqrt{\frac{m^*}{\hbar k_{1\sigma}}}\exp(ik_{1\sigma}z) + r_\sigma\sqrt{\frac{m^*}{\hbar k_{1\sigma}}}\exp(-ik_{1\sigma}z)\right], & z < 0, \\ \left[A_\sigma^{II(III,IV)}\mathrm{Ai}(-\chi_\sigma^{II(III,IV)}) + B_\sigma^{II(III,IV)} \times \mathrm{Bi}(-\chi_\sigma^{II(III,IV)})\right], & 0 \le z < L_1 + L_2 + L_3, \\ \left[t_\sigma\sqrt{\frac{m^*}{\hbar k_{5\sigma}}}\exp(ik_{5\sigma}z)\right], & z \ge L_1 + L_2 + L_3. \end{cases} \tag{2}$$

Here Ai(z) and Bi(z) are the Airy functions, $\rho = (x, y)$ is the transverse coordinate, $\mathbf{k}_{xy}$ is the in-plane wave vector

of the tunneling electrons, and

$$\chi^{II}_{\sigma_z} = \left(\frac{2m^*eF}{\hbar^2}\right)^{1/3}(z+\eta_2),\ \ \eta_2 = \left(\frac{1}{eF}\right)[E_z - V_{\sigma_z} - V_s],$$
$$\chi^{III}_{\sigma_z} = \left(\frac{2m^*eF}{\hbar^2}\right)^{1/3}(z+\eta_3),\ \eta_3 = \frac{E_z}{eF},$$
$$\chi^{IV}_{\sigma_z} = \left(\frac{2m^*eF}{\hbar^2}\right)^{1/3}(z+\eta_4),\ \ \eta_4 = \left(\frac{1}{eF}\right)[E_z - V_{\sigma_z} - V_s]. \tag{3}$$

The wave vectors outside the paramagnetic layers are given by $k_1 = \sqrt{2m^*E_z}/\hbar$ and $k_5 = \sqrt{2m^*[E_z + eF(L_1+L_2+L_3)]}/\hbar$. t_{σ_z} and r_{σ_z} are the spin-dependent transmission and reflection amplitudes of electrons, which can be calculated using the transfer-matrix method.

Our discussion of the spin-dependent shot noise is within the framework of single electron approximation and coherent tunneling, and only zero-frequency noise at $T = 4.2$ K is considered. As the standard scattering method is applied [17], we introduce creation and annihilation operators of spin-polarized electrons in the scattering states. Operators $\hat{a}^\dagger_{Ln\sigma_z}(E)$ and $\hat{a}_{Ln\sigma_z}(E)$ create and annihilate spin-σ_z electrons with total energy E in the nth channel in the left lead, which are incident upon the sample. In the same way, the creation $\hat{b}^\dagger_{Ln\sigma_z}(E)$ and annihilation $\hat{b}_{Ln\sigma_z}(E)$ operators describe electrons in the outgoing states. They obey anti-commutation relations. Therefore, we can write the scattering matrix of the sample as

$$\begin{pmatrix}\hat{b}_{Ln\sigma_z}\\ \hat{b}_{Rn\sigma_z}\end{pmatrix} = \begin{pmatrix} r_{n\sigma_z} & t'_{n\sigma_z}\\ t_{n\sigma_z} & r'_{n\sigma_z}\end{pmatrix}\begin{pmatrix}\hat{a}_{Ln\sigma_z}\\ \hat{a}_{Rn\sigma_z}\end{pmatrix} \tag{4}$$

with $t'_{n\sigma_z} = t_{n\sigma_z}$ and $r'_{n\sigma_z} = -t_{n\sigma_z}r^*_{n\sigma_z}/t^*_{n\sigma_z}$. The spin-dependent current through the lead α becomes

$$\hat{I}_{\alpha\sigma_z}(t) = \frac{e}{2\pi\hbar}\sum_{\beta\gamma}\sum_{mn}\int dEdE' e^{i(E-E')t/\hbar}\hat{a}^\dagger_{\beta m\sigma_z}(E) \times A^{mn}_{\beta\gamma}(\alpha;E,E';\sigma_z)\hat{a}_{\gamma n\sigma_z}(E'), \tag{5}$$

with the notation

$$A^{mn}_{\beta\gamma}(\alpha;E,E';\sigma_z) = \delta_{mn}\delta_{\alpha\beta}\delta_{\alpha\gamma} - \sum_k s^\dagger_{\alpha\beta;mk}(E;\sigma_z) \times s_{\alpha\gamma;kn}(E';\sigma_z). \tag{6}$$

Here s is the scattering matrix expressed in equation (4). The spin-dependent noise power is defined by

$$\begin{aligned} S_{\alpha\beta\sigma_z}(t-t') \equiv& \tfrac{1}{2}\langle\Delta\hat{I}_{\alpha\sigma_z}(t)\Delta\hat{I}_{\beta\sigma_z}(t') \\ &+ \Delta\hat{I}_{\beta\sigma_z}(t')\Delta\hat{I}_{\alpha\sigma_z}(t)\rangle, \\ 2\pi\delta(\omega+\omega')S_{\alpha\beta\sigma_z}(\omega) \equiv& \langle\Delta\hat{I}_{\alpha\sigma_z}(\omega)\Delta\hat{I}_{\beta\sigma_z}(\omega') \\ &+ \Delta\hat{I}_{\beta\sigma_z}(\omega')\Delta\hat{I}_{\alpha\sigma_z}(\omega)\rangle. \end{aligned} \tag{7}$$

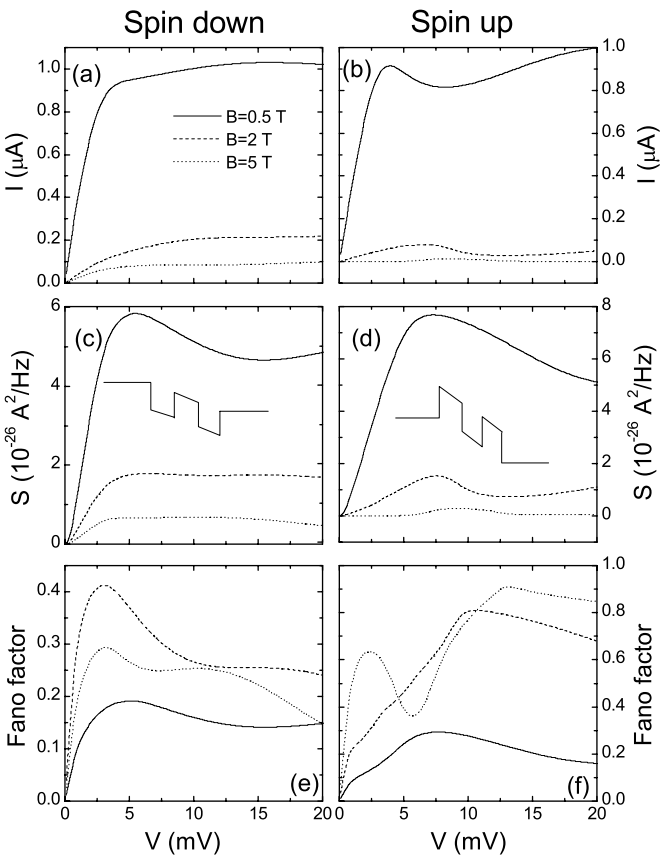

Fig. 2. Spin-dependent current as a function of the applied bias for electrons traversing asymmetric ZnSe/$Zn_{0.95}Mn_{0.05}Se$ multilayers at different external magnetic fields under positive and negative biases, respectively. $L_1 = L_2 = 10$ nm and $L_3 = 20$ nm. The insets show the potential profile for spin-up and spin-down electrons at positive and negative external biases, respectively.

In the low-frequency limit, the noise spectral density with the spin state σ_z becomes [31]

$$P_{\sigma_z} = 2\frac{e^2}{h}\int_0^\infty \{[f_1(1-f_1)+f_2(1-f_2)]\sum_n T_{n\sigma_z} + (f_1-f_2)^2\sum_n T_{n\sigma_z}(1-T_{n\sigma_z})\}dE, \tag{8}$$

where $f_1(E) = f(E-eV-E_F)$, $f_2(E) = f(E-E_F)$, f is the Fermi distribution function, and V is the bias voltage applied to the system. The spin-dependent transmission probabilities $T_{n\sigma_z} = |t_{n\sigma_z}|^2$ for the nth in-plane quantized Landau level. Here, the first two terms in equation (8) is the contribution of the thermal noise, and the third one represents the shot noise spectral density.

3 Results and discussion

We now use equation (8) to study the spin-dependent shot noise of the current for electrons traversing symmetric and

asymmetric DMS ZnSe/$Zn_{1-x}Mn_xSe$ heterostructures, where the two $Zn_{1-x}Mn_xSe$ layers have the same Mn concentration. In all of the graphs, we use $m^* = 0.16m_e$, $x = 0.05$, $N_0\alpha = 0.26$ eV, $T_0 = 1.7$ K, $V_0 = 0$ meV, $E_f = 5$ meV, and $T = 4.2$ K.

In Figure 2, we plot the spin-dependent current, shot noise, and Fano factor against the applied bias of electrons traversing symmetric ZnSe/$Zn_{1-x}Mn_xSe$ multilayers at different external magnetic fields. It can be easily seen that all physical quantities considered here are strongly dependent on the spin orientations of the tunneling electrons. It is shown that the shot noise has similar behavior to the electric current and both the spin-up and spin-down components of the shot noise are strongly suppressed as the magnetic field increases. The magnetic field increases the magnitude of the external potential energy in the Hamiltonian via Zeeman interaction and the *sp-d* exchange between the conduction-band electrons and the three-dimensional electrons of the localized magnetic moments. At a small magnetic field, the transmission for either spin-polarization is near ballistic and the *I-V* characteristic is near Ohmic with the Fano factor at an extremely small value. While the double barrier is high enough to sustain strong resonance at $B = 5$ T, the Fano factor for spin-up electrons demonstrates a sharp valley at the positive differential conductance region just before the current peak, which shows similar feature with the double-barrier heterostructures [32]. While the depth of the double well increases, the transmission is smaller for $B = 2$ T than for $B = 5$ T for spin-down electrons and the Fano factor goes inversely proportional to the transmission. This is due to that the quasi-bound resonant levels in the double-well potential profile for spin-down electrons move to lower energies for $B = 5$ T case, which enhances tunneling.

At zero bias the magnetic-induced potential is a double well for spin-down electrons or a double barrier for spin-up ones. As the magnetic field increases, the potential in the paramagnetic layers goes up for spin-up electrons and goes down for spin-down ones, so one can see that the shot noise is strongly spin-dependent and varied by the potential change.

To demonstrate the influence of the structural configuration on the shot noise, we present the spin-dependent current, shot noise, and Fano factor for electrons traversing asymmetric ZnSe/$Zn_{1-x}Mn_xSe$ multilayers at different external magnetic fields in Figures 3–5. The solid, dashed, and dotted lines correspond to $B = 0.5$, 2 and 5 T cases, respectively. It was found that transmission resonances can be enhanced to optimal resonances for spin-up electrons tunneling through the asymmetric structure with double paramagnetic layers under a certain positive bias, while for spin-down ones tunneling through the same structure, resonances can also be enhanced to optimal resonances under a certain negative bias [14]. Transmission suppression and enhancement (originating from magnetic- and electric-field-induced and structure-tuned potentials) also affect the shot noise behavior and the Fano factor. Compared with the symmetric structure, the current of spin-down electrons is enhanced and the shot noise is drastically suppressed in the asymmetric structure due to resonant enhancement in the asymmetric well structures [14] (compare Figs. 3–5 to Fig 2). At all magnetic fields the Fano factor for spin-up electrons under the positive bias is smaller than that under the negative bias due to the resonance enhancement. At a positive bias, the spin-up electrons tunnel through the thinner barrier first, while they

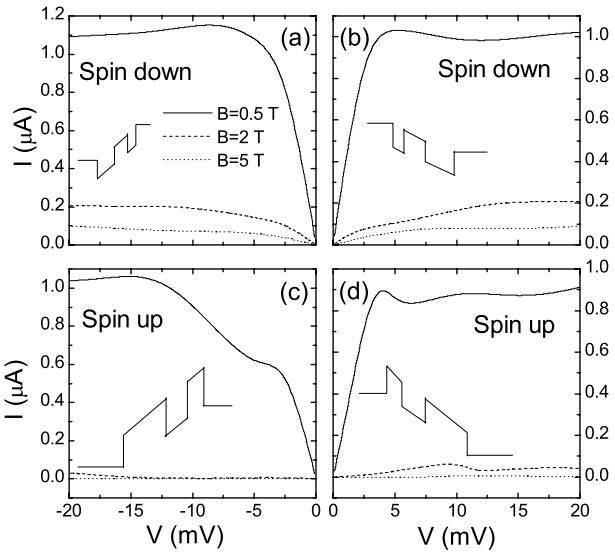

Fig. 3. Spin-dependent current as a function of the applied bias for electrons traversing asymmetric ZnSe/$Zn_{0.95}Mn_{0.05}Se$ multilayers at different external magnetic fields under positive and negative biases, respectively. $L_1 = L_2 = 10$ nm and $L_3 = 20$ nm. The insets show the potential profile for spin-up and spin-down electrons at positive and negative external biases, respectively.

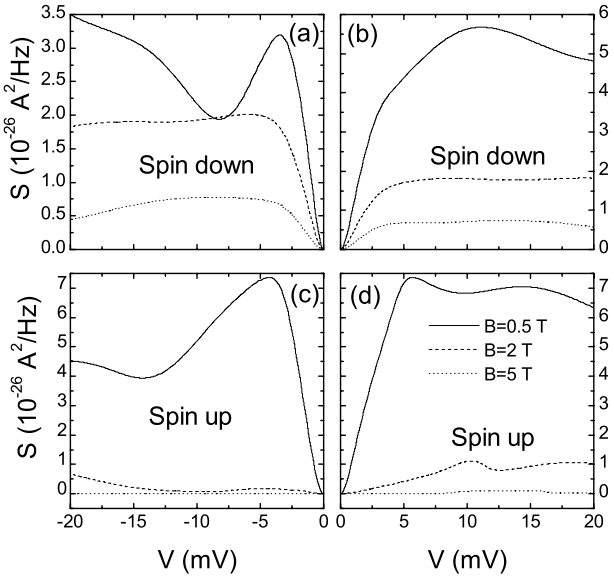

Fig. 4. Spin-dependent shot noise as a function of the applied bias for electrons traversing asymmetric ZnSe/$Zn_{0.95}Mn_{0.05}Se$ multilayers at different external magnetic fields under positive and negative biases, respectively. $L_1 = L_2 = 10$ nm and $L_3 = 20$ nm. The potential profile of each subplot is the same as that shown in Figure 3.

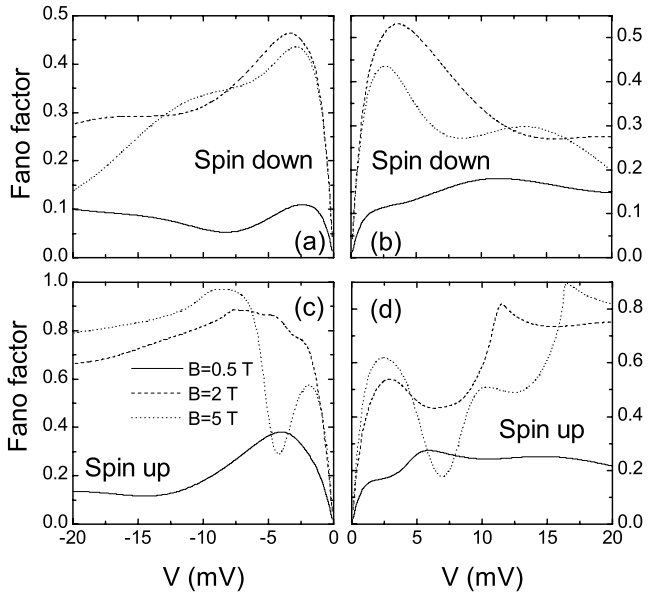

Fig. 5. Fano factor of the spin-dependent shot noise as a function of the applied bias for electrons traversing asymmetric ZnSe/$Zn_{0.95}Mn_{0.05}$Se multilayers at different external magnetic fields under positive and negative biases, respectively. $L_1 = L_2 = 10$ nm and $L_3 = 20$ nm. The potential profile of each subplot is the same as that shown in Figure 3.

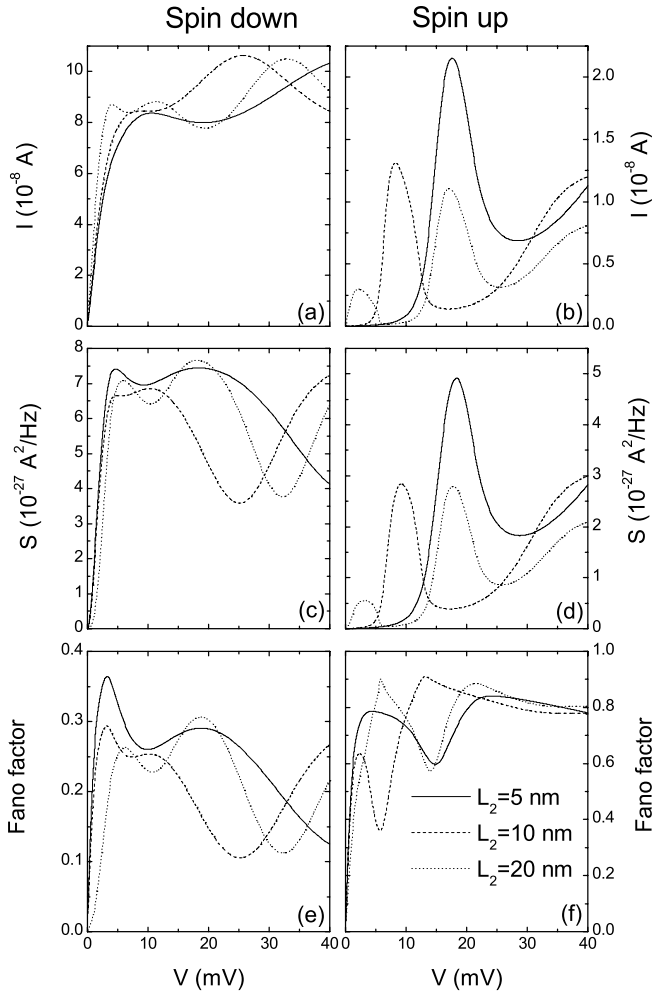

Fig. 6. Spin-dependent current, shot noise, and Fano factor for electrons traversing symmetric ZnSe/$Zn_{0.95}Mn_{0.05}$Se multilayers with different widths of nonmagnetic layers at a fixed magnetic field. $L_1 = L_3 = 10$ nm and $B = 5$ T.

tunnel through the thicker one first at a negative bias. The thicker barrier further suppresses tunneling. Thus, the transmission of the latter case is much smaller than the former case, which gives rise to smaller Fano factor of the shot noise. For the spin-down electrons, the potential profile is an asymmetric double-well structure (see the insets of Fig. 3). The quasi-bound resonant levels occur at lower energies and their intervals are smaller for a wider well. Therefore, the above case of an asymmetric double barrier for spin-up electrons is reversed. The Fano factor for spin-down electrons under the positive bias is larger than that under the negative bias at all magnetic fields. For spin-down electrons, as the magnetic field deepens the double wells, the transmission is suppressed, thus the Fano factor is increased. The transmission is smaller for $B = 2$ T than for $B = 5$ T, which induces the larger Fano factor. For spin-up electrons, the multi-resonance structure in the transmission for the double barrier is demonstrated in the multi-valley Fano factor pattern. As the magnetic field increases, more minimum valleys can be seen in the Fano factor. The similarity of tunneling mechanisms through asymmetric double-well structures and asymmetric double-barrier structures [14] demonstrates its validity in the shot noise behavior as well as in the current. Moreover, the higher-order characteristic of the system, shot noise, is more sensitive of the potential profile and system symmetry than the time-averaged current.

Since the width of the middle ZnSe layer between the double barriers/wells for spin-up/down electrons modulates the (quasi-)bound resonant states greatly, the shot noise may be modulated accordingly. In Figure 6 we present the results of the shot noise for electrons traversing symmetric ZnSe/$Zn_{1-x}Mn_x$Se multilayers with different nonmagnetic layer thickness at a fixed magnetic field. For spin-up electrons, as the width of the middle layer increases, the resonant levels in the middle well are lowered and the level intervals become narrowed. Therefore, the peak of the shot noise moves to the small bias side and develops to two peaks as the well width increases. The minimum valley of the spin-up Fano factor moves to the small-bias side with the shot noise. With the decrease of the resonant level energy, the transmission probability at a small bias is greatly enhanced, which gives rise to smaller Fano factor minimum. For spin-down electrons, as the width of the middle layer increases, the above-well virtual-state resonance becomes weaker, thus the spin-down shot noise is suppressed. For spin-up electrons, the shot noise

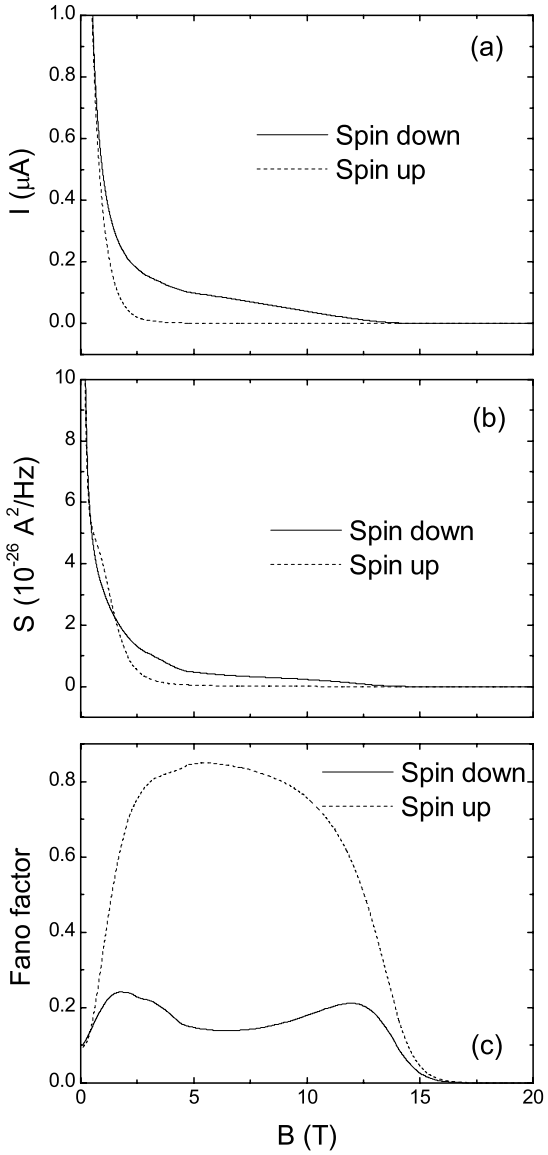

Fig. 7. Spin-dependent current, shot noise, and Fano factor for electrons traversing symmetric $ZnSe/Zn_{0.95}Mn_{0.05}Se$ multilayers as functions of the magnetic field at a fixed bias. $L_1 = L_2 = L_3 = 10$ nm and $V = 20$ mV.

peak appears at the current peak and the Fano factor minimum appears in the positive-differential-conductance regime just before the current peak, which is the characteristic of the shot noise in typical double-barrier structures. For spin-down electrons, a shot noise minimum appears at the bias where the current peak occurs and the Fano factor also shows a minimum. The largest suppression appears at medium middle-layer thickness with $L_2 = 10$ nm for both spin-up and spin-down electrons.

By varying the applied magnetic field at a fixed external bias, the magnetic field induced shot noise suppression is shown in Figure 7. The spin-dependent noise shows similar behavior to the current. As the magnetic field increases, exponential decay of the spin-up and spin-down components of the noise can be seen. The total noise is dominated by the spin-down component for fields larger than 1 T. As the transmission probability of the spin-down electrons does not decrease monotonously with the increase of the magnetic filed, a fluctuation in the Fano factor can be seen. The Fano factor becomes larger in the wide range of B for spin-up electrons and is considerably low for spin-down ones. The reason is that the transmission of the spin-up electrons is suppressed to near zero for high magnetic fields, while the suppression of the transmission of the spin-down ones occurs at a much higher magnetic field.

4 Conclusions

We reveal the relations among the shot noise in the diluted-magnetic-semiconductor/semiconductor systems with different structural configurations and under different external magnetic and electric fields. It is found that the noise shows strongly spin-dependent behavior and is affected considerably by all these internal and external conditions. The transmission properties modulated by these features cause the noticeable variations in the shot noise and Fano factor. Our results further demonstrated that the nonequilibrium fluctuations of the current measured by the shot noise are generally more sensitive to the potential profile and system symmetry than the time-averaged conductance, which may shed light on further study of the subtle mechanisms in mesoscopic transport processes.

This project was supported by the National Natural Science Foundation of China (No. 10774083), by Tsinghua Basic Research Foundation (JCpy2005058), by Specialized Research Fund for the Doctoral Program of Higher Education (No. 2006003047), and by the 973 Program (No. 2006CB605105).

References

1. S.A. Wolf, D.D. Awschalom, R.A. Buhrman, J.M. Daughton, S. von Molnar, M.L. Roukes, A.Y. Chtchelkanova, D.M. Treger, Science **294**, 1488 (2001)
2. I. Zütic, J. Fabian, S. Das Sarma, Rev. Mod. Phys. **76**, 323 (2004)
3. S.A. Wolf, A.Y. Chtchelkanova, D.M. Treger, IBM J. RES. & DEV. **50**, 101 (2006)
4. T. Hayashi, M. Tanaka, T. Nishinaga, H. Shimada, T. Tsuchiya, Y. Otuka, J. Cryst. Growth **175**, 1063 (1997)
5. H. Ohno, A. Shen, F. Matsukura, A. Oiwa, A. End, S. Katsumoto, Y. Iye, Appl. Phys. Lett. **69**, 363 (1996)
6. H. Ohno, Science **281**, 951 (1998)
7. S. Das Sarma, E.H. Hwang, A. Kaminski, Phys. Rev. B **67**, 155201 (2003)
8. H. Saito, V. Zayets, S. Yamagata, K. Ando, Phys. Rev. Lett. **90**, 207202 (2003)
9. S.S. Li, K. Chang, J.B. Xia, K. Hirose, Phys. Rev. B **68**, 245306 (2003)

10. J.C. Egues, C. Gould, G. Richter, L.W. Molenkamp, Phys. Rev. B **64**, 195319 (2001)
11. H. Munekata, H. Ohno, R.R. Ruf, R.J. Gambino, L.L. Chang, J. Cryst. Growth **111**, 1011 (1991)
12. V.I. Sugakov, S.A. Yatskevich, Sov. Tech. Phys. Lett. **18**, 134 (1992)
13. J.C. Egues, Phys. Rev. Lett. **80**, 4578 (1998)
14. Y. Guo, B.L. Gu, H. Wang, Y. Kawazoe, Phys. Rev. B **63**, 214415 (2001); Y. Guo, J.Q. Lu, B.L. Gu, Y. Kawazoe, Phys. Rev. B **64**, 155312 (2001); Y. Guo, X.Y. Chen, F. Zhai, B. L. Gu, Y. Kawazoe, Appl. Phys. Lett. **80**, 4591 (2002); Y. Guo, C.E. Shang, X.Y. Chen, Phys. Rev. B **72**, 045356 (2005)
15. M. Béjar, D. Sánchez, G. Platero, A.H. MacDonald, Phys. Rev. B **67**, 045324 (2003); D. Sánchez, A.H. MacDonald, G. Platero, Phys. Rev. B **65**, 035301 (2002); G. Papp, S. Borza, F.M. Peeters, J. Appl. Phys. **97**, 113901 (2005)
16. K. Chang, F.M. Peeters, Phys. Rev. B **68**, 205320 (2003)
17. Ya.M. Blanter, M. Buttiker, Phys. Rep. **336**, 1 (2000); R. Zhu, Y. Guo, Appl. Phys. Lett. **90**, 232104 (2007)
18. L. Saminadayar, D.C. Glattli, Y. Jin, B. Etienne, Phys. Rev. Lett. **79**, 2526 (1997)
19. F. Lefloch, C. Hoffmann, M. Sanquer, D. Quirion, Phys. Rev. Lett. **90**, 067002 (2003)
20. F.G. Brito, J.F. Estanislau, J.C. Egues, J. Magn. Magn. Mater. **226-230**, 457 (2001)
21. A. Lamacraft, Phys. Rev. B **69**, 081301 (2004)
22. M. Zareyan, W. Belzig, Europhys. Lett. **70**, 817 (2005)
23. W. Belzig, M. Zareyan, Phys. Rev. B **69**, 140407 (2004)
24. B. Wang, J. Wang, H. Guo, Phys. Rev. B **69**, 153301 (2004)
25. H. Yu, J.Q. Liang, Phys. Rev. B **72**, 075351 (2005)
26. O. Sauret, D. Feinberg, Phys. Rev. Lett. **92**, 106601 (2004)
27. J.C. Egues, G. Burkard, D. Loss, Phys. Rev. Lett. **89**, 176401 (2002)
28. J.C. Egues, G. Burkard, D.S. Saraga, J. Schliemann, D. Loss, Phys. Rev. B **72**, 235326 (2005)
29. F.G. Brito, J.C. Egues, Braz. J. Phys. **32** (2A), 324 (2002)
30. Y.X. Li, Y. Guo, B.Z. Li, Phys. Rev. B **72**, 075321 (2005)
31. M. Buttiker, Phys. Rev. B **46**, 12485 (1992)
32. V.Y. Aleshkin, L. Reggiani, M. Rosini, Phys. Rev. B **73**, 165320 (2006)